Tumor and Stem Cell Biology

Cancer Research

Cell Surface Tetraspanin Tspan8 Contributes to Molecular Pathways of Exosome-Induced Endothelial Cell Activation

Irina Nazarenko[1], Sanyukta Rana[1], Alexandra Baumann[1], Jessica McAlear[1], Andrea Hellwig[2], Michael Trendelenburg[3], Günter Lochnit[4], Klaus T. Preissner[4], and Margot Zöller[1]

Abstract

Tumor-derived exosomes containing the tetraspanin Tspan8 can efficiently induce angiogenesis in tumors and tumor-free tissues. However, little information exists on exosome–endothelial cell (EC) interactions or the proangiogenic role of tetraspanins, which are a constitutive component of exosomes. In this study, we used a rat adenocarcinoma model (AS-Tspan8) to explore the effects of exosomal Tspan8 on angiogenesis. Tspan8 contributed to a selective recruitment of proteins and mRNA into exosomes, including CD106 and CD49d, which were implicated in exosome-EC binding and EC internalization. We found that EC internalized Tspan8-CD49d complex–containing exosomes. Exosome uptake induced vascular endothelial growth factor (VEGF)–independent regulation of several angiogenesis-related genes, including *von Willebrand factor, Tspan8*, chemokines *CXCL5* and *MIF*, chemokine receptor *CCR1*, and, together with VEGF, *VEGF receptor 2*. EC uptake of Tspan8-CD49d complex–containing exosomes was accompanied by enhanced EC proliferation, migration, sprouting, and maturation of EC progenitors. Unraveling these new pathways of exosome-initiated EC regulation could provide new options for therapeutic interference with tumor-induced angiogenesis. *Cancer Res; 70(4); 1668–78. ©2010 AACR.*

Introduction

Rapidly growing solid tumors depend on angiogenesis, initiated by dominance of proangiogenic factors (1, 2). We recently identified the tetraspanin Tspan8 (formerly D6.1A/CO-029) as an important angiogenesis inducer within the tumor and tumor-free tissue, which can culminate in disseminated intravascular coagulation (DIC; refs. 3, 4). The cross talk between a tumor and its environment has been intensively explored (5). Systemic tumor-induced alterations, like the thrombotic state, are poorly understood (6) but suggested to require soluble mediators (7). Recently, exosomes have come into focus as potent intercellular communicators (8, 9). Tetraspanins being enriched in exosomes (10, 11), we hypothesized that tumor-derived Tspan8 exosomes contribute to systemic angiogenesis.

Exosomes, 50- to 100-nm vesicles, derived from endosomes forming multivesicular bodies, are abundantly released by tumor cells (8, 12, 13). Primary sources of endosomes are caveolae, clathrin-coated pits, and tetraspanin-enriched microdomains (TEM; ref. 13). These types of membrane microdomains are also recovered in exosomes (8, 14, 15). Additionally, exosomes contain selectively enriched mRNA and miRNA that regulate gene expression in target cells (16). Indeed, the source of exosomes defines their function. Antigen-presenting cell–derived exosomes induce and tumor-derived exosomes suppress an immune response (17).

The recovery of membrane microdomains in exosomes is of particular interest with respect to tetraspanins, which organize clusters of tetraspanins, additional transmembrane proteins, and membrane-proximal signaling proteins, such as integrins, G protein–coupled receptors, proteases, and protein kinase C (10, 18–20). Prominent Tspan8 partners are CD13, EWI-F, intersectin-2, EpCAM, CD49c, and CD104 (21). Within TEM, tetraspanins act as "molecular facilitators" (10, 18), getting involved in cell motility, adhesion (10, 20–23), scaffolding of signal transduction molecules (10, 18, 21), vesicle, and cell fusion (10, 18, 24). Based on these features, tetraspanins might well become involved in exosome-recipient cell binding, which proceeds via receptor-ligand interaction, fusion, or internalization (8, 13, 17, 25). The restriction of the exosome-target cell interaction (13, 16) relies on the exosomal proteins and target cell ligands (21).

Authors' Affiliations: [1]Department of Tumor Cell Biology, University Hospital of Surgery; [2]Interdisciplinary Center for Neurosciences, University of Heidelberg; [3]Department of Cell Biology, German Cancer Research Center, Heidelberg, Germany and [4]Institute of Biochemistry, University of Giessen, Giessen, Germany

Note: Supplementary data for this article are available at Cancer Research Online (http://cancerres.aacrjournals.org/).

S. Rana, A. Baumann, J. McAlear, and A. Hellwig performed experiments; G. Lochnit, K.T. Preissner, and M. Trendelenburg designed, performed, and analyzed experiments; I. Nazarenko designed, performed, and analyzed experiments and contributed to writing; M. Zöller designed and analyzed experiments and wrote the manuscript.

Corresponding Authors: Margot Zöller, Department of Tumor Cell Biology, University Hospital of Surgery, Im Neuenheimer Feld 365, D-69120 Heidelberg, Germany. Phone: 49-6221-565146; Fax: 49-6221-565199; E-mail: m.zoeller@dkfz.de or Irina Nazarenko, Karlsruhe Institute of Technology, Institute of Toxicology and Genetics, Hermann-von-Helmholtz-Platz 1, D-7634 Eggenstein-Leopoldshafen, Germany. Phone: 49-7247-823302; E-mail: irina.nazarenko@kit.edu.

doi: 10.1158/0008-5472.CAN-09-2470

Tumor-derived exosomes are present in body fluids (26) and likely are involved in systemic angiogenesis, which can culminate in severe thrombosis (27). Therefore, a blockade of angiogenesis-initiating exosomes may hinder tumor vascularization and thrombosis, sparing physiologic, angiogenic factor–initiated angiogenesis. As a precondition for therapeutic interference, we started to evaluate components and activity of angiogenesis-initiating AS-Tspan8 exosomes (4). We show that a Tspan8-CD49d association contributes to exosome binding to endothelial cell (EC) and identified potential pathways, whereby internalized exosomes can modulate the fate of EC and EC progenitors (ECP).

Materials and Methods

Rats, tumors, and primary cells. BDX rats were kept under specific pathogen-free conditions (animal facilities, German Cancer Research Center). BSp73AS (AS; BDX-derived pancreatic adenocarcinoma) cells (28), AS-Tspan8 clones (4), lung fibroblasts (LuFb), and rat aortic ECs (RAEC; CellLining) were maintained in RPMI 1640/10% FCS. Primary aortic ring (AoR; 1-mm-thick slices)–derived EC and ECP were cultured in MCDB131 or RPMI 1640/2% FCS, 2 mmol/L glutamine, 1 μg/mL hydrocortisone, and 5 units/mL heparin with or without 0.1% EC supplement (Sigma). ECs were enriched using biotinylated lectin (Sigma) and streptavidin-conjugated dynabeads (Invitrogen). Purity was controlled by anti-CD31 staining.

Antibodies. Primary antibodies are listed in Supplementary Table S1. Hybridoma-derived antibodies were FITC or rhodamine labeled. Biotinylated, horseradish peroxidase (HRP)–conjugated, and fluorochrome-conjugated secondary antibodies were obtained commercially (BD Pharmingen, Dianova, and Biotrend).

RNA and reverse transcription-PCR. Exosomal and cellular mRNA was extracted using RNeasy Mini kit (Qiagen). Transcription and amplification followed routine procedure. Amplified gene products were semiquantitatively evaluated (ImageJ freeware). Real-time PCR was performed using SYBR PCR kit (Qiagen), StepOne Real-Time PCR System, and statistical analysis by the ΔC_t method according to the supplier's recommendation (Applied Biosystems). Primers are listed in Supplementary Table S2.

Microarray mRNA analysis. Expression levels of 22,523 rat transcripts were analyzed using Illumina RatRef-12 chip in duplicates. Analyses, normalization, and statistics were performed at the Core Facility, German Cancer Research Center. Cellular and exosomal samples were normalized independently. Transcripts with at least double signal intensity over background, bead SE differences of >12, and P value of <0.05 were included. mRNAs that differed in AS versus AS-Tspan8 exosomes by >3-fold and in AS exosome–treated versus AS-Tspan8 exosome–treated RAEC by >1.5-fold were considered as differentially expressed. The microarray analysis series record is GSE18812.[5]

Flow cytometry. Flow cytometry (1×10^5 to 3×10^5 cells per sample) followed routine procedures. Trypsinized cells were allowed to recover (2 h, 37°C, RPMI 1640/10% FCS). Samples were analyzed by a FACSCalibur (BD Biosciences).

Immunofluorescence. Cells on coverslips were fixed, permeabilized, blocked, incubated with primary antibodies (2–10 μg/mL, 60 min, 4°C) and fluorochrome-conjugated secondary antibodies (60 min, 4°C), blocked, incubated with second dye-labeled antibodies (60 min, 4°C) and washed. Coverslips were mounted in Elvanol. Digitized images (Carl Zeiss LSM710 confocal microscope) were generated. For topology analysis, 12 Z-stack images were taken in 1-μm steps. Focus plane was adjusted visually and three-dimensional projection was generated. For all applications, AxioVision Software Rel. 4.7 was used.

Exosome preparation. Cells were cultured (36 h) in serum-free medium. Cleared supernatants (2 × 10 min, 500 × g; 1 × 20 min, 2,000 × g; 1 × 30 min, 10,000 × g) were centrifuged (90 min, 100,000 × g) and washed (PBS, 90 min, 100,000 × g). Crude exosome preparations were suspended in 2.5 mol/L sucrose, overlaid by a continuous sucrose gradient (0.25–2 mol/L), and centrifuged (15 h, 150,000 × g). Where indicated, exosomes were prepared after cell biotinylation (45 min, 4°C) or rhodamine-DHPE labeling (60 min, 4°C). Relative fluorescence intensity was evaluated at 540-nm excitation and 590-nm emission and adjusted to rhodamine-DHPE standards.

Proteome analysis. Exosomal proteins (700 μg/analysis/duplicate) were subjected to two-dimensional electrophoresis or prehydrated plastic sheet gel strips for separation of hydrophobic proteins (29) followed by matrix-assisted laser desorption/ionization–time-of-flight analysis. Densitometric analyses were done with the PDQuest software after Flamingo staining (Bio-Rad).

Biotinylation, immunoprecipitation, and Western blot. Cells were washed in HEPES buffer and, where required, incubated with 0.1 mg/mL water-soluble sulfo-NHS-biotin (30 min, 4°C). Cells were lysed (HEPES buffer, 1% Lubrol, 1 mmol/L phenylmethylsulfonyl fluoride, protease inhibitor mix) for 30 min at 4°C. For immunoprecipitation, lysates were incubated with the indicated antibody (2 h) and protein G–Sepharose (1 h). After washing (four times), lysates/immunoprecipitates were resolved on 12% nonreducing SDS-PAGE and subjected to immunoblotting using HRP-conjugated antibody/streptavidin following enhanced chemiluminescence–based signal detection.

Migration assays. Subconfluent monolayers were scratched (wound) and evaluated after 24 to 72 h by light microscopy. For Transwell migration (Boyden chambers, 8-μm pore size membranes), cells were added to the upper (1×10^6/mL, RPMI 1640/0.1% FCS) and to the lower [RPMI 1640/10% FCS, 10 μg/mL exosomes or 5 ng/mL vascular endothelial growth factor (VEGF)] chamber. After 12 h, cells on the lower membrane side were fixed and crystal violet stained (595-nm absorbance).

[5] http://www.ncbi.nlm.nih.gov/geo/query/acc.cgi?acc=GSE18812

Matrigel assay. Freshly cut AoR and AoR-EC were embedded in Matrigel (24-well plates) and covered with RPMI 1640/2% FCS, 5 ng/mL VEGF, or 10 μg/mL exosomes. Cable formation was evaluated after 12 d (AoR) or 1 d (AoR-EC) by light microscopy.

Proliferation assay. ECs were incubated for 24 to 96 h in RPMI 1640/2% FCS, 5 ng/mL VEGF, or 10 μg/mL exosomes. [^{3}H]Thymidine was added during the last 16 h. [^{3}H]Thymidine incorporation was measured in a β-counter.

Statistics. According to request, assays (three repetitions, regardless of intra-assay triplicates) were statistically evaluated by the two-tailed Student's *t* test, Kruskal-Wallis test, or Mann-Whitney test. *P* values of <0.05 were considered significant.

Results

AS-Tspan8 cells induce angiogenesis (3, 4). AS-Tspan8 exosomes, but neither AS exosomes nor exosome-depleted AS-Tspan8 supernatant, induce EC sprouting (4). A Tspan8-expressing metastatic subline does not induce angiogenesis (28), indicating that exosomal Tspan8 is required but not sufficient for angiogenesis induction. Thus, the questions arose on the particular features allowing AS-Tspan8 exosomes, which do not contain VEGF, to initiate EC activation.

AS-Tspan8 exosome characterization. Crude exosome preparations of both AS and AS-Tspan8 cells contained 30 to 50 μg protein/100 mL supernatant, suggesting that AS-Tspan8–initiated angiogenesis unlikely is due to abundance of AS-Tspan8 exosomes compared with AS exosomes. To avoid impurities, revealed by electron microscopy (Supplementary Fig. S1), we performed sucrose density gradient centrifugation, resulting in a yield of 4 to 8 μg protein/100 mL supernatant. Western blot analysis showed enrichment of tetraspanins and the exosome markers CD71, heat shock protein (HSP) 70, and Lamp1 in the 1.141- to 1.171-day fractions. Tetraspanin nonassociated Bag6 served as a control (Fig. 1A).

To obtain information toward the content of AS-Tspan8 exosomes compared with AS exosomes, we proceeded with

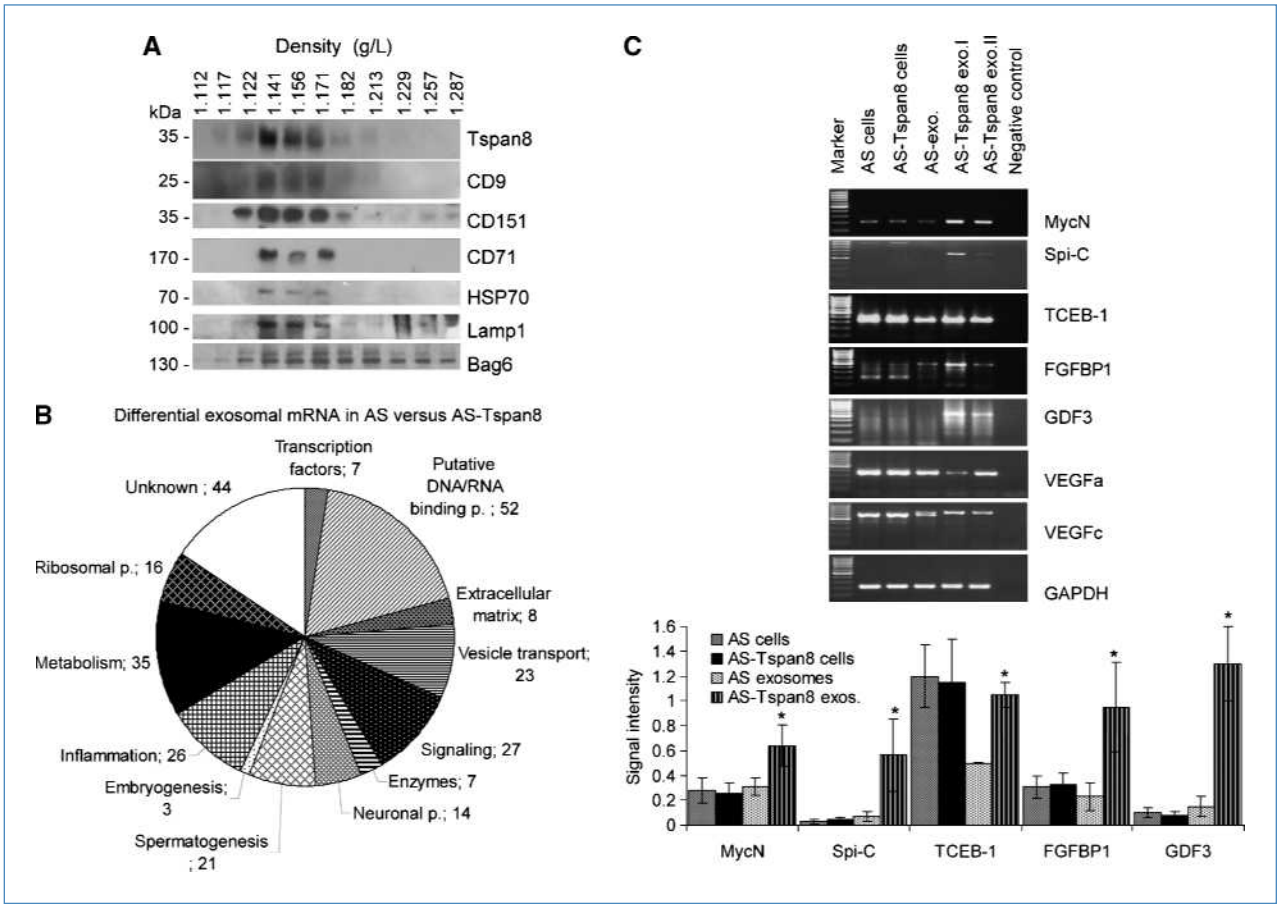

Figure 1. Differential mRNA analysis of AS and AS-Tspan8 exosomes. A, Western blot of sucrose density gradient fractions of exosomes. Tspan8, CD9, CD151, CD71, HSP70, and Lamp1 (exosomal proteins) are recovered in the day 1.141 to day 1.171 fractions; control: Bag6. B, categories of 285 mRNAs enriched in AS-Tspan8 exosomes: overview (details: Supplementary Table S3). C, RT-PCR verification of candidate genes and semiquantitative evaluation (mean of three experiments). *, significant increase in AS-Tspan8 exosomes.

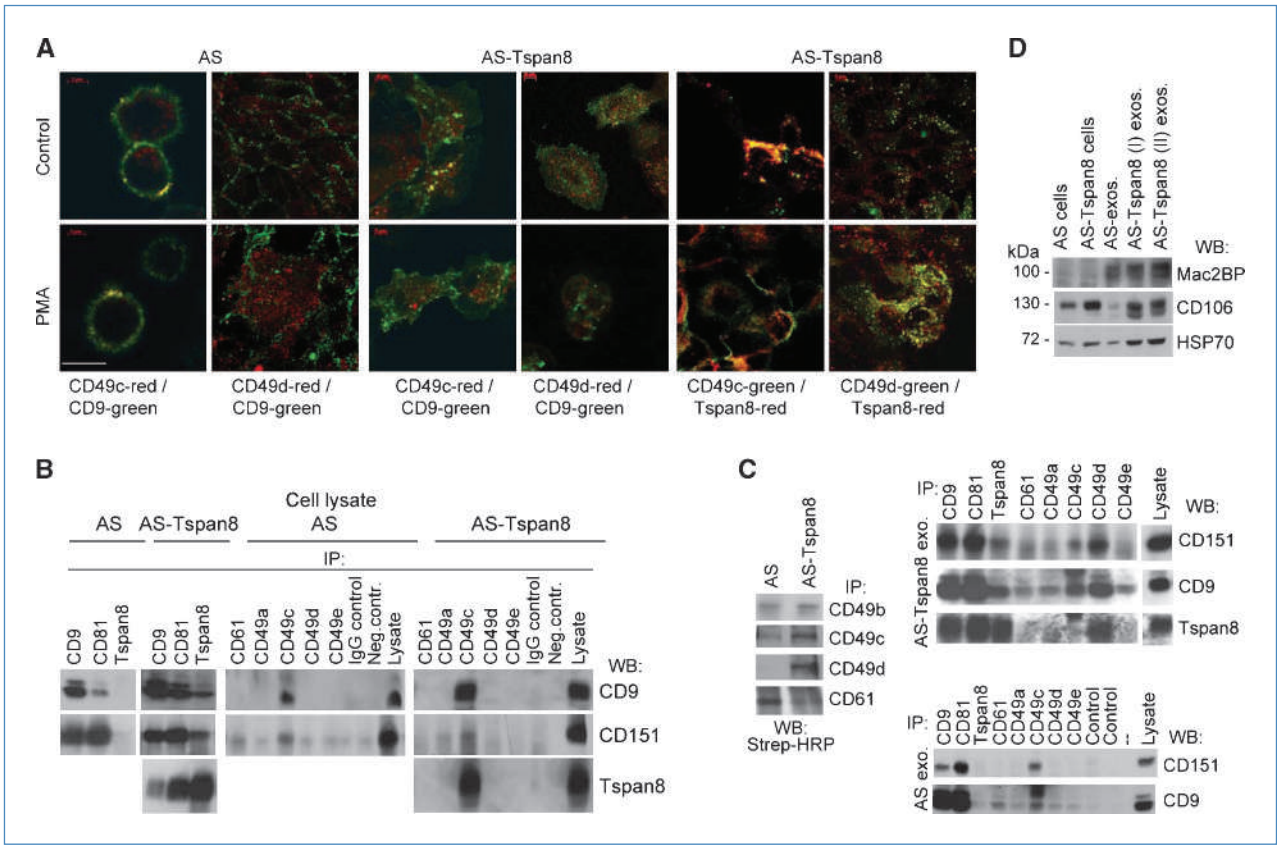

Figure 2. Distinct tetraspanin webs in AS and AS-Tspan8 exosomes. A, immunofluorescence of AS and AS-Tspan8 cells. CD49c weakly colocalizes with CD9 but strongly with Tspan8. Colocalization remains unaltered after PMA treatment. Only Tspan8 colocalizes with CD49d. Colocalization becomes strengthened after internalization. Scale bar, 20 μm. B, coimmunoprecipitation of tetraspanins and integrins in AS and AS-Tspan8 cell lysates: CD9, CD151, and Tspan8 (AS-Tspan8) coimmunoprecipitate mutually and with CD49c. C, immunoprecipitation of exosomal integrins: AS and AS-Tspan8 exosomes contain CD49b, CD49c, and CD61. Only AS-Tspan8 exosomes contain CD49d. Tetraspanins mutually coimmunoprecipitate in AS and AS-Tspan8 exosomes. In AS exosomes, CD49c coimmunoprecipitates with CD9 and CD151; CD61 and CD49e coimmunoprecipitate with CD9. In AS-Tspan8 exosomes, CD49d coimmunoprecipitates with CD9, CD151, and Tspan8; CD49c coimmunoprecipitates with CD9 and CD151 but not Tspan8. D, Western blot of Mac2BP, CD106, and HSP70 in AS and AS-Tspan8 cells and exosome lysates: the three proteins are enriched in AS-Tspan8 exosomes.

a differential analysis of exosomal mRNA and proteins using two AS and AS-Tspan8 exosome preparations, the latter being derived from two clones with comparable levels of Tspan8 (Supplementary Fig. S2).

AS and AS-Tspan8 exosomes contained ~1,500 transcripts; 285 were enriched by >3-fold in AS-Tspan8 exosomes (Supplementary Table S3; Fig. 1B). Being particularly interested in transcription factors, vesicle transporters, and signaling molecules, enhanced expression of the transcription factors *MycN, Spi-C, elongation factor B(SIII)*, *TCEB-1, fibroblast growth factor binding protein 1* (*FGFBP1*), and *growth and differentiation factor-3* (*GDF3*) was verified in AS-Tspan8 exosomes compared with AS exosomes and the parental cells by reverse transcription-PCR (RT-PCR). *VEGF* mRNA was not enriched in AS-Tspan8 cells or exosomes (Fig. 1C). *CCL20, prothrombin, bone morphogenetic protein-2, several Ras* and *mitogen-activated protein kinase family members*, and a *phosphatase 2A subunit* were below the detection level (data not shown).

Tetraspanins act by modulating the activities of associated proteins, major partners being integrins. Exosomes deriving from internalized membrane domains, we first evaluated tetraspanin and integrin colocalization at the cell membrane and after phorbol 12-myristate 13-acetate (PMA)–induced internalization. CD49c colocalization with CD9 and Tspan8 remained unaltered after internalization. In contrast, CD49d weakly colocalized with CD9 and Tspan8 at the cell membrane but only with Tspan8 after internalization (Fig. 2A). In cell lysates, Tspan8 coimmunoprecipitated with CD9, CD151, and CD49c. CD49c also coimmunoprecipitated with CD9 (Fig. 2B). Coimmunoprecipitation differed in exosomes. CD49c, CD49b, and CD61 were recovered in AS and AS-Tspan8 exosomes. CD49d and CD49e were only present in AS-Tspan8 exosomes, suggesting their selective recruitment. CD49c and CD61 coimmunoprecipitated with CD9 in AS and AS-Tspan8 exosome lysates. CD49e coimmunoprecipitated with CD9. Instead, CD49d coimmunoprecipitated with CD9, CD151, and Tspan8 only in AS-Tspan8 exosome lysates,

which suggests a rearrangement of the Tspan8 web during internalization (Fig. 2C).

A comparative proteome analysis revealed, besides the distinctly recruited CD49d, high recovery of minichromosome maintenance protein 7 (MCM7), laminin receptor 1 (lamininR1), Mac2BP (galactoside binding protein-3), CD106/VCAM-1, HSP70, and the major VAULT protein in AS-Tspan8 exosomes (Supplementary Table S4). CD106, HSP70, and Mac2BP enrichment was confirmed by Western blot (Fig. 2D).

These results show that Tspan8 overexpression in AS cells has a major effect on the recruitment of selected proteins and mRNA into exosomes. We next elaborated whether exosomal Tspan8 contributes to EC targeting.

AS-Tspan8 exosome binding to and uptake by EC. Immunofluorescence of RAEC incubated with dye-labeled AS-Tspan8 exosomes showed a higher binding rate of AS-Tspan8 than AS exosomes, and a three-dimensional analysis indicated internalization of the dye-labeled exosomes. D6.1 (anti-rat Tspan8), anti-CD49d, and anti-CD106 inhibited AS-Tspan8 exosome binding to RAEC but not to LuFb. Low binding of AS exosomes by RAEC was not inhibited. Instead, anti-CD151 and anti-CD49c inhibited both AS and AS-Tspan8 exosome binding by LuFb; anti-CD9 inhibited AS exosome binding (Fig. 3A and B).

To further evaluate exosome incorporation, biotinylated AS/AS-Tspan8 exosomes were cocultured with AoR-EC or

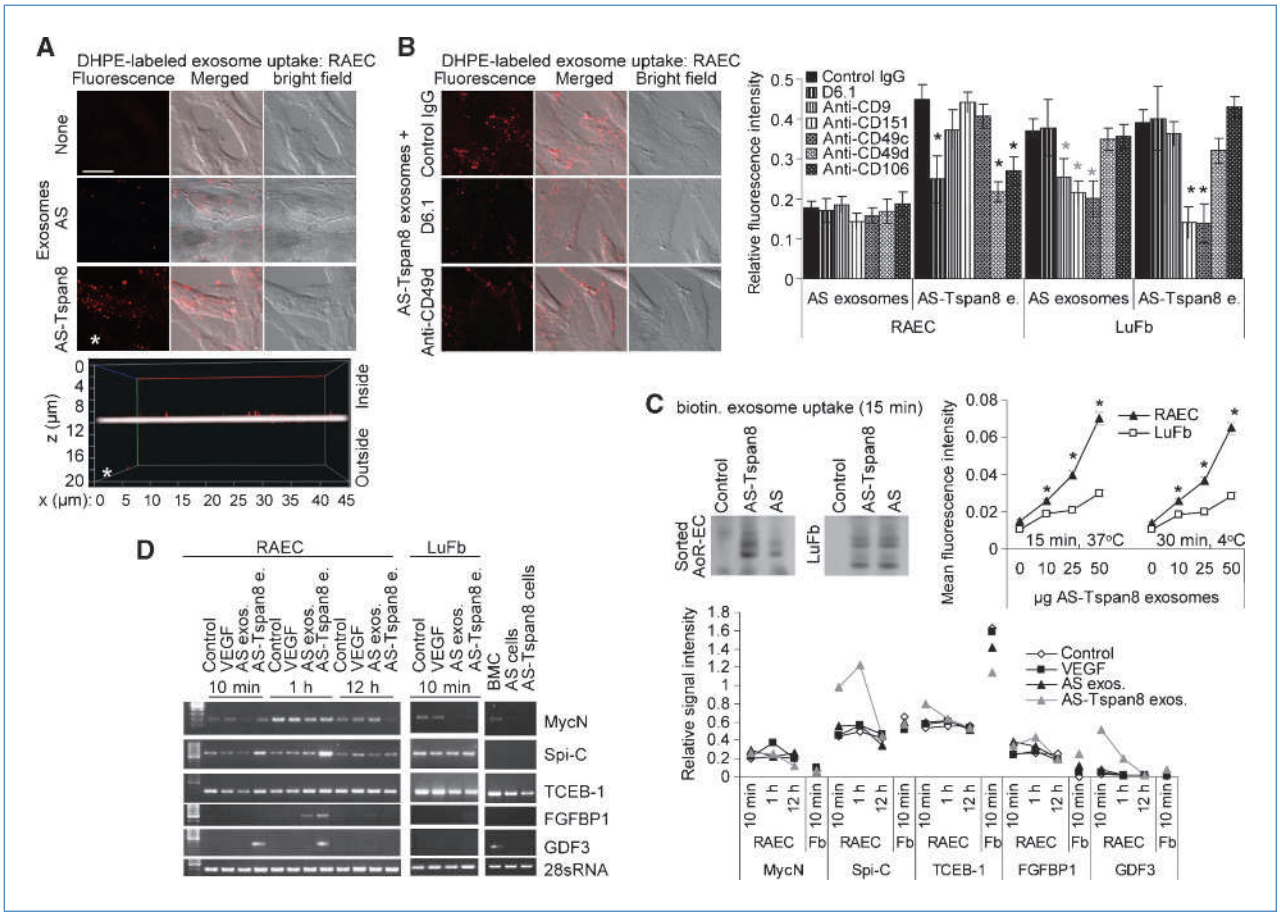

Figure 3. Exosome attachment and uptake by EC. A, DHPE-labeled AS and AS-Tspan8 exosomes were incubated with RAEC (15 min, 37°C). Confocal microscopy of fluorescent exosome binding (fluorescence, light field, overlay, scale bar: 10 μm); Z-stack plane (*) showed AS-Tspan8 exosome signals within the cell membrane and on the inner membrane side. B, RAEC and LuFb binding of DHPE-labeled AS-Tspan8 exosomes (15 min, 37°C) after exosome preincubation with antibody (20 μg/mL): confocal microscopy (fluorescence, light field, overlay). After washing and lysis, exosome uptake was measured in an ELISA reader. D6.1, anti-CD49d, and anti-CD106 inhibited AS-Tspan8 exosome uptake by RAEC. Anti-CD151, anti-CD49c, and anti-CD9 inhibited AS and AS-Tspan8 exosome uptake by LuFb. C, RAEC and LuFb were incubated with biotinylated exosomes. Lysates of washed cells were separated (SDS-PAGE), transferred, and blotted with streptavidin-HRP. Biotinylated protein profiles were similar in LuFb incubated with AS and AS-Tspan8 exosomes. Instead, higher amounts of biotinylated proteins were recovered in RAEC incubated with AS-Tspan8 exosomes. Titrated amounts of DHPE-labeled AS-Tspan8 exosomes were incubated (15 min, 37°C or 30 min, 4°C) with RAEC or LuFb. Only in RAEC, AS-Tspan8 exosome uptake increases with exosome concentration. B and C, mean values ± SD of triplicates. *, significant differences between AS and AS-Tspan8 exosomes. D, RT-PCR (one of three experiments) from RAEC and LuFb mRNA after coculture with VEGF, AS exosomes, or AS-Tspan8 exosomes (100 μg/mL) for 10 min, 1 h, or 12 h. MycN, Spi-C, TCEB-1, FGFBP1, and GDF3 mRNAs were transiently recovered in RAEC but not LuFb. Controls: BMC, AS, and AS-Tspan8 mRNA and 28S RNA.

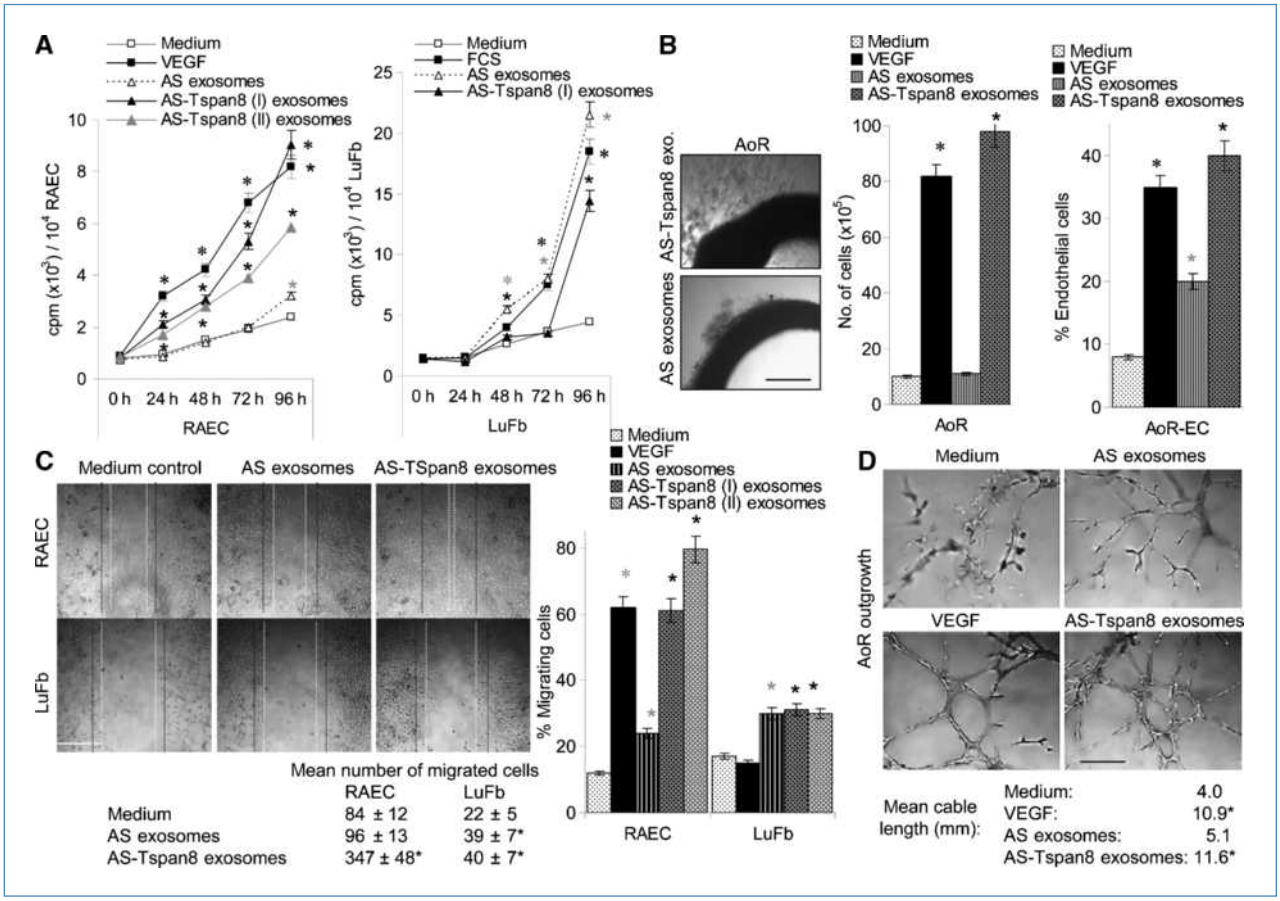

Figure 4. AS-Tspan8 exosome–promoted EC proliferation and migration. A, RAEC and LuFb were cocultured with VEGF, AS exosomes, or AS-Tspan8 exosomes (10 μg/mL). Proliferative activity (triplicates, mean ± SD) was evaluated by [^{3}H]thymidine uptake after 24 to 96 h. B, microscopic appearance (scale bar: 500 μm), cell recovery (mean ± SD of 10 fields, five independent cultures), and percentage of FITC-Dio-Ac-LDL$^+$ cells (flow cytometry) of AoR cultured for 2 wk in RPMI 1640/10% FCS, VEGF, AS exosomes, or AS-Tspan8 exosomes (20 μg/mL). The recovery of EC was increased after coculture with AS-Tspan8 exosomes. C, RAEC and LuFb monolayers were scratched; medium was exchanged as indicated; wound healing was evaluated after 48 h. Black dotted line, scratch; white dotted line, healing (scale bar: 500 μm); mean ± SD (10 fields, three independent cultures) of migrated cells. Cells (RPMI 1640/0.1% FCS) were seeded in the upper chamber of Transwell plates. The lower chamber contained RPMI 1640/10% FCS (control) and the indicated supplements. Absorbance (595 nm) of crystal violet–stained cells was measured after 24 h. The percentage of migrating cells (triplicates, mean ± SD) is shown. AS-Tspan8 exosomes accelerated RAEC but not LuFb migration. D, Matrigel-embedded AoR outgrowths were cocultured with exosomes or VEGF: cable-like structures (scale bar: 1mm) and mean ± SD cable length (10 fields) after 12 d. VEGF and AS-Tspan8 exosomes support cable-like growth and branching. *, significant differences between AS and AS-Tspan8 exosomes.

LuFb. Cells were lysed, and proteins were separated by SDS-PAGE, transferred, and stained with streptavidin-HRP. LuFb and AoR-EC incorporated exosome-derived biotin. Whereas identical biotinylated protein patterns were recovered in LuFb, AoR-EC preferentially incorporated AS-Tspan8 exosomes. Adding dye-labeled AS-Tspan8 exosomes to RAEC and LuFb, fluorescent dye recovery in RAEC linearly increased with the amount of exosomes. Low dye recovery in LuFb indicated modest uptake (Fig. 3C).

EC also incorporated exosomal mRNA. *Spi-C, GDF3*, and *FGFBP1* mRNA, enriched in AS-Tspan8 exosomes, were transferred into RAEC but not, or weakly, into LuFb. Genes were recovered after 10 minutes to 1 hour of coincubation, but not after 12 hours, suggesting a short lifetime of transferred mRNA. Notably, these mRNAs were below detection level in AS-Tspan8 cells, confirming selective enrichment in AS-Tspan8 exosomes (Fig. 3D).

These findings provide evidence for pronounced AS-Tspan8 exosome binding and uptake by EC, which involves Tspan8 and CD49d and may be strengthened by CD106.

Tspan8 exosomes initiate activation of resting EC and maturation of ECP. When purified exosomes were cultured with RAEC and LuFb, AS-Tspan8 exosomes and VEGF induced stronger RAEC proliferation than AS exosomes. AS exosomes supported LuFb proliferation (Fig. 4A). AS-Tspan8 exosomes sufficed to activate resting EC from quiescent AoR as efficiently as VEGF. Dio-Ac-LDL uptake revealed that the percentage of outgrowing EC was particularly increased. AS exosomes induced a minor increase in EC compared with untreated controls (Fig. 4B).

AS-Tspan8 exosomes also supported pronounced migration of RAEC in wound healing and Transwell migration (Fig. 4C). When embedded in Matrigel, AoR outgrowth formed a larger network and AoR-EC showed stronger branching in cocultures with VEGF and AS-Tspan8 than AS exosomes (Fig. 4D; Supplementary Fig. S3B). To control for Tspan8 exosome selectivity, AoR-EC migration and sprouting on Matrigel was evaluated with exosomes from additional rat tumor cell lines, AT6.1, AT6.1-Tspan8, BDX2, and MatLyLu. Except MatLyLu, the lines express CD49d, but only AT6.1-Tspan8 and BDX2 express Tspan8 (Supplementary Fig. S2B). Only exosomes derived from Tspan8-expressing cells accelerated migration and cable formation (Supplementary Fig. S3A and B), confirming a role of Tspan8 in exosome-initiated EC activation.

Proliferation and migration of EC cocultured with AS-Tspan8 exosomes was accompanied by regulation of gene expression. A genome-wide mRNA screening revealed several genes in EC, triggered selectively by AS-Tspan8 exosomes (Supplementary Table S5). Validation via RT-PCR confirmed strong *CXCL5, CCR1, MIF*, and *DEC1* (*deleted in esophageal cancer*) induction in RAEC by AS-Tspan8 exosomes; *HMOX1* (*hemoxygenase 1*), *VEGF receptor 1* (*VEGFR1*), *von Willebrand factor* (*vWF*), and *tissue factor* (*TF*) expression was induced by AS-Tspan8 exosomes and *VEGF. CXCL5, TF*, and *HMOX1* expression was also regulated in LuFb (Fig. 5A). Elevated mRNA levels remained stable or increased during 120 hours of coculture (data not shown). Transcription of Tspan8 was observed after 48 hours and increased until 72 to 120 hours of coculture. A synergistic effect of VEGF and AS-Tspan8 exosomes was observed on *VEGFR2* expression. Confirming the AS-Tspan8 exosome specificity, transcription of other genes, such as *smooth muscle actin* (*SMA*), was not affected (Fig. 5B).

Early ECPs are defined by clonal expansion and the potential to differentiate into ECs and smooth muscle cells (SMC; Supplementary Fig. S4; ref. 30). When cocultured with VEGF, only few AoR outgrowths survived for more than five passages. These cells showed the appearance of EC confirmed by Dio-Ac-LDL uptake. Instead, in the presence of low amounts (0.1 μg/mL) of AS-Tspan8 exosomes, a population of clustered, densely packed, small round cells became visible

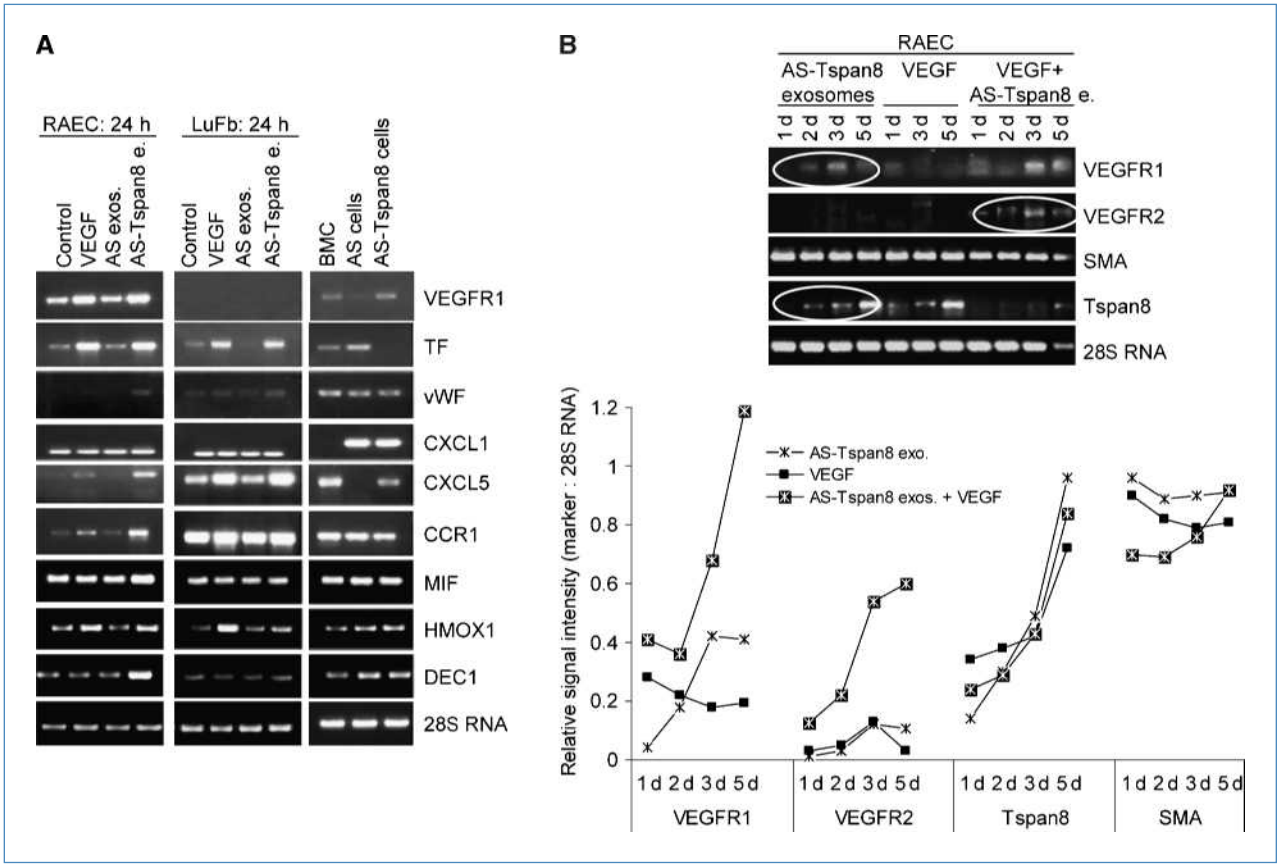

Figure 5. AS-Tspan8 exosome–initiated angiogenic switch. A, RT-PCR of RAEC and LuFb after coculture with VEGF, AS exosomes, or AS-Tspan8 exosomes (100 μg/mL) for 24 h; controls: BMC, AS, and AS-Tspan8 mRNA. AS-Tspan8 exosomes induced VEGFR1, TF, weakly vWF, CXCL1, CXCL5, CCR1, MIF, HMOX1, and DEC1 transcription in RAEC. TF and CXCL5 transcription was also induced in LuFb. B, RT-PCR and signal strength quantification for VEGFR1, VEGFR2, SMA, and Tspan8 of RAEC cocultured for 1 to 5 d with AS-Tspan8 exosomes and/or VEGF. AS-Tspan8 exosome–induced VEGFR1 transcription increased with time. AS-Tspan8 exosomes and VEGF induced Tspan8 transcription only after 3 to 5 d. Induction of VEGFR2 transcription required AS-Tspan8 exosomes plus VEGF.

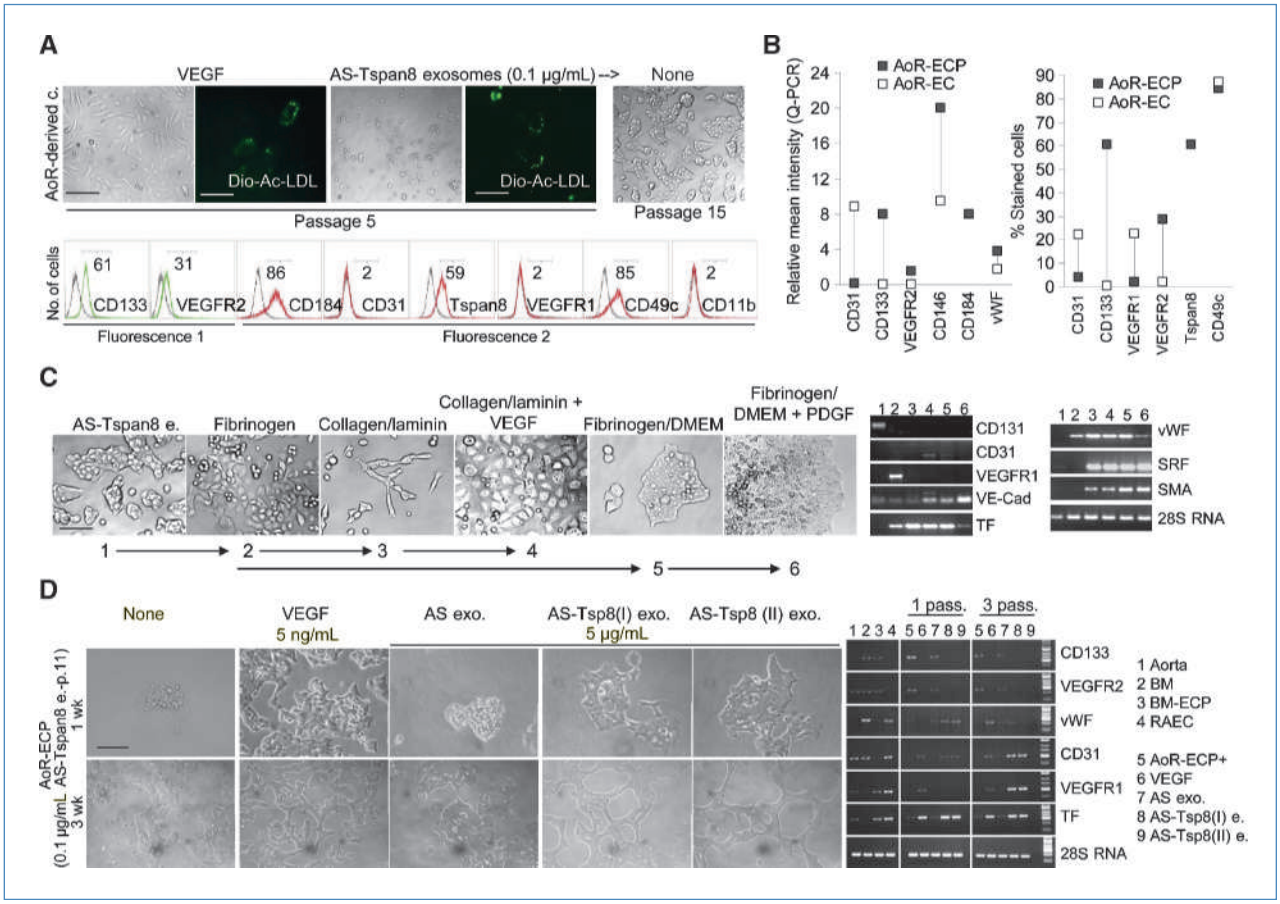

Figure 6. AS-Tspan8 exosome–initiated ECP maturation. A, microscopic appearance (scale bar: 200 µm) and Dio-Ac-LDL uptake (scale bar: 50 µm) of the 5th and 15th passages of AoR outgrowth cocultured with VEGF or AS-Tspan8 exosomes (0.1 µg/mL). Only AS-Tspan8 exosome–containing cultures developed clusters of round, densely packed cells that partly took up Dio-Ac-LDL and showed the expression profile (flow cytometry, fifth passage) of ECP. Cells were maintained with unaltered morphology for >3 mo. B, gene expression after 11 passages in comparison with AoR-EC. Left, quantitative PCR; right, flow cytometry. ECP are $CD31^-$ and $VEGFR1^-$, $CD133^+$, $CD146^+$, $CD184^+$, $Tspan8^+$, $VEGFR2^{low}$, and vWF^{low}. C, ECPs (fifth passage) were seeded on fibrinogen-coated or collagen-coated plus laminin-coated plates with or without VEGF or cultured in DMEM on fibrinogen-coated plates with or without PDGF: morphology (scale bar: 200 µm) and CD131, CD31, VEGFR1, VE-cadherin, TF, vWF, SRF, and SMA expression (RT-PCR). CD131 expression was lost under all culture conditions; fibrinogen promoted VEGFR1, TF, and vWF expression. Fibrinogen/DMEM strengthened TF and vWF and induced VE-cadherin, SRF, and SMA expression; VEGFR1 expression was lost. PDGF strengthened VE-cadherin, SRF, and SMA and weakened TF and vWF expression. Collagen/laminin induced TF, vWF, SRF, and SMA expression. VEGF induced CD31, VE-cadherin, TF, vWF, and SRF expression. D, cells (11th passage) were seeded on gelatin-coated plates and cocultured for one to three passages with 5 µg/mL AS or AS-Tspan8 exosomes or VEGF: morphology (scale bar: 100 µm) and gene expression (RT-PCR) after one and three passages in comparison with RAEC, BMC, and BMC-derived ECP (31). In cocultures with 5 µg/mL AS-Tspan8 exosomes, ECPs start to form cable-like structures, lose CD133 and VEGFR2, but gain CD31 and VEGFR1 expression, resembling mature ECs.

after 4 to 6 weeks (five passages). These cells were $CD133^+$, $CD184^+$, $Tspan8^+$, $CD49c^+$, $VEGFR2^{low}$, $CD31^-$, $VEGFR1^-$, and $CD11b^-$ and partly took up Dio-Ac-LDL. They could be maintained in MCDB131 medium in the absence of AS-Tspan8 exosomes for >15 passages (Fig. 6A). As compared with mature ECs, cells from the 11th passage, analyzed by quantitative PCR and flow cytometry, showed higher CD133, VEGFR2, CD146, and vWF expression; high CD184 and Tspan8; but lower CD31 and VEGFR1 and unaltered CD49c expression (Fig. 6B). To further control for the suggested nature of ECP, cells from the fifth passage were exposed to selective culture conditions, known to promote ECP differentiation. On passaging on fibrinogen, they expressed *VEGFR1, TF,* and *vWF*. When passaged on a collagen/laminin mixture together with VEGF, cells acquired the cobblestone phenotype of differentiated EC; *CD31* expression was induced, *TF* expression was strengthened, and *VEGFR1* expression was lost. In the presence of fibrinogen plus platelet-derived growth factor (PDGF), cells strongly proliferated, exhibited reduced *TF* and *vWF* expression, but impressively produced *serum response factor* (*SRF*) and SMA (Fig. 6C).

Having shown selection and maintenance of ECP with differentiation potential from AoR in the presence of low-level AS-Tspan8 exosomes, we asked whether these cells can be driven into differentiation by higher AS-Tspan8 exosome concentrations. Cells were cultured on gelatin-coated plates

for three passages in the presence of 5 μg/mL AS or AS-Tspan8 exosomes or 5 ng/mL VEGF. Both VEGF and AS-Tspan8 exosomes, but not AS exosomes, induced formation of cable-like structures, loss of *CD133* and *VEGFR2*, but upregulation of *CD31, VEGFR1*, and *TF* expression, acquiring an expression profile similar to mature AoR-EC. RAEC, bone marrow cell (BMC), and BMC-derived ECP (31) served as controls (Fig. 6D).

Thus, exosomes can bind to EC and potentially ECP via Tspan8-associated CD49d. Exosomes become internalized and exosomal proteins and/or mRNA induce gene expression that suffices for activation of quiescent EC. AS-Tspan8 exosomes also allow for survival of ECP. ECP can be driven into EC and SM differentiation depending on the environment or toward mature EC by AS-Tspan8 exosomes.

Discussion

AS-Tspan8 exosomes strongly affect angiogenesis. As selective interference with tumor angiogenesis would provide a powerful therapeutics (32), AS-Tspan8 exosomes could become a most interesting carrier. Therefore, we started to unravel their activity.

Exosomal Tspan8 and Tspan8-associated proteins initiate EC activation. AS tumors are vascularized, but do not induce DIC. AS-Tspan8 tumors are highly vascularized and induce DIC. Abundantly Tspan8-expressing ASML tumors are poorly vascularized (3, 28). These three tumors strongly express CD9, CD81, and CD151 (3, 4, 33). Coimmunoprecipitation of Tspan8 with integrins revealed that, in ASML cells, Tspan8 interacts with CD104 and overexpression of CD104 in AS-Tspan8 cells prevents angiogenesis (34). These findings indicated that selective integrin associations with Tspan8 might be decisive for Tspan8 exosome–induced angiogenesis.

Indeed, comparing Tspan8 associations in AS-Tspan8 exosomes and CD9 associations in AS and AS-Tspan8 exosomes revealed that CD49d associates with CD9, CD151, and Tspan8 only in AS-Tspan8 exosomes. In contrast, CD49c associates with CD9 in both AS and AS-Tspan8 exosomes. This implies that Tspan8 selectively recruits CD49d into exosomes via yet unknown mechanisms.

The presence of Tspan8-associated CD49d is utmost important for AS-Tspan8 exosome–induced EC activation. Whereas AS and AS-Tspan8 exosomes bind and become internalized with comparable efficacy by fibroblasts, AS-Tspan8 exosomes bind with far higher efficacy than AS exosomes to EC. Only AS-Tspan8 exosome binding/uptake by EC is inhibited by D6.1 and anti-CD49d, whereas anti-CD49c or anti-CD151 inhibit binding/uptake of AS and AS-Tspan8 exosomes by fibroblasts. As only D6.1 inhibits exosome binding/uptake by EC, although CD49d coimmunoprecipitates in AS-Tspan8 exosome lysates with CD9, CD151, and Tspan8, we suggest that only Tspan8-associated CD49d contributes to exosome-EC interactions, where the Tspan8-CD49d complex could mediate firm adhesion.

A proteome analysis revealed that from 12 proteins enriched in AS-Tspan8 exosomes, 4 were adhesion molecules: CD106, lamininR1, Mac2BP, and milk fat globule epidermal growth factor 8 protein (MFGE8). Their contribution to AS-Tspan8 exosome uptake remains to be explored. CD106 is a CD49d ligand on EC, involved in reticulocyte-derived exosome binding to fibronectin (35), and also might contribute by binding to CD49d on EC. Its involvement is supported by anti-CD106 inhibiting AS-Tspan8 exosome uptake. Mac2BP regulates cell adhesion and binds to endosialin, selectively expressed by tumor vasculature (36, 37). In AS-Tspan8 exosomes, it may support EC binding. MFGE8, found in exosome-like vesicles, binds $\alpha_v\beta_3$ and $\alpha_v\beta_5$ and is involved in apoptotic cell clearance (38). LamininR1 is engaged in adhesion, signal transduction, and matrix metalloproteinase (MMP) 2 activation (39). Experiments are in progress to control for these activities in AS-Tspan8 exosome–induced angiogenesis.

Additional AS-Tspan8 exosome–enriched proteins possibly support EC survival. The major VAULT protein is important in drug resistance (40). CD71 regulates proliferation and angiogenesis (41). HSPs are constitutively enriched in exosomes (42) and exosomal HSP70 protects neurons from stress damage (43). The minichromosome maintenance complex member MCM7, highly expressed in many malignancies, is at the core of the DNA replication process (44). Its transfer via exosomes could support DNA replication in proliferating EC.

Most of these proteins are frequently recovered in exosomes (42). One reason for their enrichment in AS-Tspan8 exosomes could rely on peculiarities of Tspan8 internalization. Tspan8, distinct from CD9 and CD151, may become, at least partly, internalized via clathrin-coated pits.[6] Selective features of Tspan8 internalization/recruitment into exosomes could explain the different protein composition of AS-Tspan8 versus AS exosomes.

Taken together, Tspan8 exosomes interact with EC. The Tspan8 association with CD49d likely supports persisting binding/uptake. LamininR1, Mac2BP, and MFGE8 may contribute to this selective interaction. Abundance of proteases CD13 and MMPs (data not shown) in AS-Tspan8 exosomes could facilitate the integration process. The major VAULT protein CD71 and HSP70 might provide survival advantages.

Differential mRNA recovery in AS-Tspan8 exosomes and altered protein and mRNA recovery in EC. AS-Tspan8 and AS exosome mRNA profiles differ considerably. From 11 mRNAs expected to be relevant in targeted EC, elevated levels were confirmed for 5 mRNAs: the oncogene MycN, the transcription factor Spi-C, the transcription elongation factor ElonginC, GDF3, and FGFBP1. The angiogenic switch molecule FGFBP1 (45) and the nodal-like transforming growth factor-β ligand GDF3 (46) are of special interest considering the angiogenic activity of AS-Tspan8 exosomes. Both genes were transiently recovered in EC after coculture with AS-Tspan8 exosomes, confirming AS-Tspan8 exosome integration in EC.

Strengthening our hypothesis that Tspan8 exosomes initiate a VEGF-independent proangiogenic pathway, VEGF protein (4) and mRNA recovery were poor in AS-Tspan8

[6] S. Rana, unpublished data.

exosomes. In addition, angiopoietin-1, angiopoietin-2, Tie-1, and Tie-2 RNAs were not or poorly recovered (data not shown).

Thus, exosomal mRNA becomes transferred and likely contributes to AS-Tspan8 exosome–induced angiogenesis.

AS-Tspan8 exosome–initiated ECP maturation and angiogenesis-related gene expression. Although AS-Tspan8 exosomes do not contain angiogenic factors, AoR-ECs respond with proliferation and cord formation comparable with VEGF. AS-Tspan8 exosomes, but not VEGF, suffice for long-term survival of ECP, which could be driven by additional factors into mature EC or SMC, but also can acquire an EC-like phenotype by exposure to AS-Tspan8 exosomes. Thus, AS-Tspan8 exosomes possess the potential to regulate ECP in adults and possibly during embryogenesis. This is in line with exosome-like argosomes acting as morphogen transporters (13, 41, 47) and abundant Tspan8 expression in vessel endothelium during embryogenesis (48).

Induction of EC migration correlates with CCR1, CCL20, CXCL5, and MIF expression on coculture of EC with AS-Tspan8 exosomes. MIF promotes angiogenic growth factor expression, possibly by hypoxia-inducible factor-1α stabilization (49), and stimulates MMP3 (50), expression of which was also induced by AS-Tspan8 exosomes. Induced transcription of angiopoietin-like 4 and a cDNA with similarity to vWF may support the angiogenic switch. The effects of cDNA, coding for signal transduction molecules and transcription factors, remain to be explored; EC proliferation could well rely on their abundance. On prolonged coculture, VEGFR1, TF, vWF, Tspan8, and, in the presence of VEGF, VEGFR2 are transcribed, which complements motility-related gene expression in promoting EC proliferation and differentiation.

Altogether, dependent on their origin, exosomes induce angiogenesis without an initial requirement for known angiogenic factors. They also support survival, expansion, and maturation of ECP. Tetraspanins are consistently recovered in exosomes (13, 21, 42), yet there had been no clue for their exosomal activity. We show that tetraspanins can be a central component for exosome binding and integration into distinct target cells. For EC, one of the "master" molecules is Tspan8 as long as the originating cell expresses appropriate cooperating partners, such as CD49d. We will proceed with a comprehensive definition of angiogenesis-promoting and angiogenesis-inhibiting proteins, mRNA and miRNA, whose integration into exosomes becomes guided by Tspan8 and modulates EC fate. Tspan8 exosomes playing a central role in tumor-induced local and systemic angiogenesis, modulated exosomes could possibly become a highly effective antiangiogenic drug, whereas *ex vivo* expansion of undifferentiated ECP could serve as a tool in reconstructive medicine.

Disclosure of Potential Conflicts of Interest

No potential conflicts of interest were disclosed.

Acknowledgments

We thank H. Bading (Center for Neurosciences, University of Heidelberg) for providing electron microscopy facility and S. Poppelreuther (Zeiss Core-Facility, Heidelberg, Germany) for help with confocal microscopy.

Grant Support

SPP1190 (M. Zöller), Tumorzentrum-Heidelberg/Mannheim (M. Zöller), and Käthe und Josef Klinz-Stiftung (I. Nazarenko). I. Nazarenko is currently supported by the European Social Fund and Ministry of Science, Research and Arts, Baden-Württemberg.

The costs of publication of this article were defrayed in part by the payment of page charges. This article must therefore be hereby marked *advertisement* in accordance with 18 U.S.C. Section 1734 solely to indicate this fact.

Received 7/2/09; revised 12/8/09; accepted 12/9/09; published OnlineFirst 2/2/10.

References

1. Kerbel RS. Tumor angiogenesis. N Engl J Med 2008;358:2039–49.
2. Roskoski R, Jr. Vascular endothelial growth factor (VEGF) signaling in tumor progression. Crit Rev Oncol Hematol 2007;62:179–213.
3. Claas C, Seiter S, Claas A, Savelyeva L, Schwab M, Zöller M. Association between the rat homologue of CO-029, a metastasis-associated tetraspanin molecule and consumption coagulopathy. J Cell Biol 1998;141:267–80.
4. Gesierich S, Berezovskiy I, Ryschich E, Zöller M. Systemic induction of the angiogenesis switch by the tetraspanin D6.1A/CO-029. Cancer Res 2006;66:7083–94.
5. Acker T, Plate KH. Role of hypoxia in tumor angiogenesis-molecular and cellular angiogenic crosstalk. Cell Tissue Res 2003;314:145–55.
6. Zwicker JI, Furie BC, Furie B. Cancer-associated thrombosis. Crit Rev Oncol Hematol 2007;62:126–36.
7. Re RN, Cook JL. An intracrine view of angiogenesis. Bioessays 2006; 28:943–53.
8. Février B, Raposo G. Exosomes: endosomal-derived vesicles shipping extracellular messages. Curr Opin Cell Biol 2004;16:415–21.
9. Johnstone RM. Exosomes biological significance: a concise review. Blood Cells Mol Dis 2006;36:315–21.
10. Hemler ME. Tetraspanin functions and associated microdomains. Nat Rev Mol Cell Biol 2005;6:801–11.
11. Zöller M. Gastrointestinal tumors: metastasis and tetraspanins. Z Gastroenterol 2006;44:573–86.
12. de Gassart A, Géminard C, Hoekstra D, Vidal M. Exosome secretion: the art of reutilizing nonrecycled proteins? Traffic 2004;5:896–903.
13. Lakkaraju A, Rodriguez-Boulan E. Itinerant exosomes: emerging roles in cell and tissue polarity. Trends Cell Biol 2008;18:199–209.
14. Calzolari A, Raggi C, Deaglio S, et al. TfR2 localizes in lipid raft domains and is released in exosomes to activate signal transduction along the MAPK pathway. J Cell Sci 2006;119:4486–98.
15. Trajkovic K, Hsu C, Chiantia S, et al. Ceramide triggers budding of exosome vesicles into multivesicular endosomes. Science 2008;319: 1244–7.
16. Valadi H, Ekström K, Bossios A, Sjöstrand M, Lee JJ, Lötvall JO. Exosome-mediated transfer of mRNAs and microRNAs is a novel mechanism of genetic exchange between cells. Nat Cell Biol 2007; 9:654–9.
17. Schorey JS, Bhatnagar S. Exosome function: from tumor immunology to pathogen biology. Traffic 2008;9:871–81.

18. Levy S, Shoham T. The tetraspanin web modulates immune-signalling complexes. Nat Rev Immunol 2005;5:136–48.
19. Le Naour F, André M, Boucheix C, Rubinstein E. Membrane microdomains and proteomics: lessons from tetraspanin microdomains and comparison with lipid rafts. Proteomics 2006;6:6447–54.
20. Berditchevski F. Complexes of tetraspanins with integrins: more than meets the eye. J Cell Sci 2001;114:4143–51.
21. Zöller M. Tetraspanins: push and pull in suppressing and promoting metastasis. Nat Rev Cancer 2009;9:40–55.
22. Winterwood NE, Varzavand A, Meland MN, Ashman LK, Stipp CS. A critical role for tetraspanin CD151 in α3β1 and α6β4 integrin-dependent tumor cell functions on laminin-5. Mol Biol Cell 2006; 17:2707–21.
23. Zijlstra A, Lewis J, Degryse B, Stuhlmann H, Quigley JP. The inhibition of tumor cell intravasation and subsequent metastasis via regulation of *in vivo* tumor cell motility by the tetraspanin CD151. Cancer Cell 2008;13:221–34.
24. Vjugina U, Evans JP. New insights into the molecular basis of mammalian sperm-egg membrane interactions. Front Biosci 2008; 13:462–76.
25. Lebreton A, Séraphin B. Exosome-mediated quality control: substrate recruitment and molecular activity. Biochim Biophys Acta 2008;1779:558–65.
26. Simpson RJ, Lim JW, Moritz RL, Mathivanan S. Exosomes: proteomic insights and diagnostic potential. Expert Rev Proteomics 2009;6: 267–83.
27. Sood SL. Cancer-associated thrombosis. Curr Opin Hematol 2009; 16:378–85.
28. Matzku S, Komitowski D, Mildenberger M, Zöller M. Characterization of BSp73, a spontaneous rat tumor and its *in vivo* selected variants showing different metastasizing capacities. Invasion Metastasis 1983;3:109–23.
29. Wenge B, Bönisch H, Grabitzki J, Lochnit G, Schmitz B, Ahrend MH. Separation of membrane proteins by two-dimensional electrophoresis using cationic rehydrated strips. Electrophoresis 2008;29:1511–7.
30. Kubo H, Alitalo K. The bloody fate of endothelial stem cells. Genes Dev 2003;17:322–9.
31. Kähler CM, Wechselberger J, Hilbe W, et al. Peripheral infusion of rat bone marrow derived endothelial progenitor cells leads to homing in acute lung injury. Respir Res 2007;8:50.
32. Loges S, Mazzone M, Hohensinner P, Carmeliet P. Silencing or fueling metastasis with VEGF inhibitors: antiangiogenesis revisited. Cancer Cell 2009;15:167–70.
33. Claas C, Wahl J, Orlicky DJ, et al. The tetraspanin D6.1A and its molecular partners on rat carcinoma cells. Biochem J 2005;389:99–110.
34. Herlevsen M, Schmidt DS, Miyazaki K, Zöller M. The association of the tetraspanin D6.1A with the α6β4 integrin supports cell motility and liver metastasis formation. J Cell Sci 2003;116:4373–90.
35. Rieu S, Géminard C, Rabesandratana H, Sainte-Marie J, Vidal M. Exosomes released during reticulocyte maturation bind to fibronectin via integrin α4β1. Eur J Biochem 2000;267:583–90.
36. Park YP, Choi SC, Kim BY, et al. Induction of Mac-2BP by nerve growth factor is regulated by the PI3K/Akt/NF-κB-dependent pathway in the HEK293 cell line. BMB Rep 2008;41:784–9.
37. Teicher BA. Newer vascular targets: endosialin (review). Int J Oncol 2007;30:305–12.
38. Aoki N. Regulation and functional relevance of milk fat globules and their components in the mammary gland. Biosci Biotechnol Biochem 2006;70:2019–27.
39. Nelson J, McFerran NV, Pivato G, et al. The 67 kDa laminin receptor: structure, function and role in disease. Biosci Rep 2008;28:33–48.
40. Berger W, Steiner E, Grusch M, Elbling L, Micksche M. Vaults and the major vault protein: novel roles in signal pathway regulation and immunity. Cell Mol Life Sci 2009;66:43–61.
41. Szekeres T, Sedlak J, Novotny L. Benzamide riboside, a recent inhibitor of inosine 5′-monophosphate dehydrogenase induces transferrin receptors in cancer cells. Curr Med Chem 2002;9:759–64.
42. Simpson RJ, Jensen SS, Lim JW. Proteomic profiling of exosomes: current perspectives. Proteomics 2008;8:4083–99.
43. Taylor AR, Robinson MB, Gifondorwa DJ, Tytell M, Milligan CE. Regulation of heat shock protein 70 release in astrocytes: role of signaling kinases. Dev Neurobiol 2007;67:1815–29.
44. Costa A, Onesti S. The MCM complex: (just) a replicative helicase? Biochem Soc Trans 2008;36:136–40.
45. Abuharbeid S, Czubayko F, Aigner A. The fibroblast growth factor-binding protein FGF-BP. Int J Biochem Cell Biol 2006;38:1463–8.
46. Levine AJ, Brivanlou AH. GDF3 at the crossroads of TGF-β signaling. Cell Cycle 2006;5:1069–73.
47. Dieterlen-Lièvre F, Jaffredo T. Decoding the hemogenic endothelium in mammals. Cell Stem Cell 2009;4:189–90.
48. Claas C, Herrmann K, Matzku S, Möller P, Zöller M. Developmentally regulated expression of metastasis-associated antigens in the rat. Cell Growth Differ 1996;7:663–78.
49. Rendon BE, Willer SS, Zundel W, Mitchell RA. Mechanisms of macrophage migration inhibitory factor (MIF)-dependent tumor microenvironmental adaptation. Exp Mol Pathol 2009;86:180–5.
50. Nishihira J, Ishibashi T, Fukushima T, Sun B, Sato Y, Todo S. Macrophage migration inhibitory factor (MIF): its potential role in tumor growth and tumor-associated angiogenesis. Ann N Y Acad Sci 2003;995:171–82.